İSTANBUL UNIVERSITY CERRAHPAŞA

ORIGINAL ARTICLE
Electrica 2023; 23(2): 151-159

Comparison of Interior Mounted Permanent Magnet Synchronous Motor Drives with Sinusoidal, Third Harmonic Injection, and Space Vector Pulse Width Modulation Strategies with particular attention to Current Distortions and Torque Ripples

Osman Emre Özçiflikçi, Mikail Koç

Department of Electrical-Electronic Engineering, Kırşehir Ahi Evran University, Faculty of Engineering-Architecture, Kırşehir, Turkey

Cite this article as: O. E. Özçiflikçi and M. Koç, "Comparison of interior mounted permanent magnet synchronous motor drives with sinusoidal, third harmonic injection, and space vector pulse width modulation strategies in particular attention to current distortions and torque ripples," *Electrica*, 23(2), 151-159, 2023.

ABSTRACT

Interior Mounted Permanent Magnet Synchronous Motors (IPMs) have become popular in electric vehicle traction applications in recent years due to their superior features such as high efficiency and high power density compared to other machines. Therefore, development of IPM drive systems is an important research area. In this study, three different pulse width modulation (PWM) strategies commonly used in machine drives are compared extensively in IPM drives. Simulations have been carried out with optimum dq-axes currents based on demanded torque from the system, and hence, the simulated drives are efficiency-optimized. Sinusoidal pulse width modulation (SPWM), third harmonic injection pulse width modulation (THIPWM), and space vector pulse width modulation (SVPWM) strategies have been employed in the drives, and comparisons have been made by paying particular attention to the total harmonic distortion (THD) rates of phase currents and torque ripples. It has been validated through extensive simulations that the SVPWM strategy has less THD percentage for IPM drives than SPWM and THIPWM at wide operating points, and hence, the current and torque responses are better with smooth output torque. Simulation results also validate that the current distortions and torque ripples are the highest when SPWM strategy is adopted in the drives, and hence, the THIPWM strategy is superior to the SPWM.

***Index Terms*—**Interior Mounted Permanent Magnet Synchronous Motors, sinusoidal pulse width modulation, space vector pulse width modulation, total harmonic distortion, third harmonic injection pulse width modulation

I. INTRODUCTION

Permanent magnet synchronous machines (PMSM) are frequently used in areas such as electric vehicles and railway systems due to their superior features such as high efficiency, high power density, low acoustic noise and controllability in a wide speed range [1, 2]. Permanent magnet synchronous machines can be broadly divided into two groups, the Surface Mounted Permanent Magnet Synchronous Motor (SPM) and the Interior Mounted Permanent Magnet Synchronous Motor (IPM) [3]. Due to the saliency on the rotor of the IPMs, the torque density is higher as IPMs have the capacity to produce reluctance torque in addition to the magnet torque.

Field-oriented control (FOC) and direct torque control (DTC) techniques are commonly used in the control of AC drives [4]. In both the FOC and DTC techniques, the input of the system is the electromagnetic torque or speed command. However, while the FOC technique works with the principle of driving current errors to zero by comparing the command currents generated in the controller with the measured dq-axes current values fed from the motor phases [5], in the DTC technique, the electromagnetic torque and the stator flux magnitude errors are driven to zero where an observer is a must to estimate the actual values of torque and flux [6]. The DTC technique uses flux and torque observers for feedback control. In low-speed regions where the voltage values are low, the performance of the observers may deteriorate, which greatly reduces the performance of the DTC system [7]. In hysteresis-based DTC drives, phase current distortions and torque ripples considerably increases and the use of hysteresis comparators in DTC technique causes variable switching frequency and therefore requires more sampling time than other control techniques [8]. To solve this problem, DTC technique can be implemented using pulse width modulation (PWM) techniques [9]. Similarly, in the FOC technique, three-phase motors are driven

Corresponding author:
Osman Emre Özçiflikçi

E-mail:
osman.ozciflikci@ahievran.edu.tr

Received: March 1, 2022

Revised: May 30, 2022

Accepted: June 5, 2022

Publication Date: September 26, 2022

DOI: 10.5152/electrica.2022.22035

by employing PWM strategies. In other words, PWM strategies have an all-around advantage in AC motor drives. Output torque production can be obtained with lower ripple with the development of PWM strategies and hence smoother currents and electromagnetic torque can be achieved.

Three different types of PWM are commonly used in the literature, namely sinusoidal PWM (SPWM) [10, 11], third harmonic injection PWM (THIPWM) [12, 13], and space vector PWM (SVPWM) [14-16]. Sinusoidal PWM strategy is frequently used in motor drives because it is simple and easy to implement. However, it is not an efficient strategy due to low DC link utilization rate, high switching losses, and high current distortions for motor drive systems. Although the high-definition SPWM strategy is applied in [17] to reduce the harmonics and computational burden of the SPWM strategy with smoother outputs, the low DC link utilization rate is still a major drawback for motor drives. The THIPWM strategy is an alternative technique to increase the DC link voltage utilization level. Even though the THIPWM strategy is a PWM strategy based on the SPWM strategy, its DC link utilization rate is about 15.5% higher than SPWM. Space vector pulse width modulation strategy is frequently used in recent motor drives due to its superior features such as high DC link utilization rate, low switching losses, and low total harmonic distortion (THD) rates. In addition, there are studies in the literature on reducing the computational burden of SVPWM and providing less switching losses [18, 19].

Sinusoidal pulse width modulation and THIPWM strategies have been compared in terms of THD and DC link utilization rate in [13]; however, the resultant influence on a motor drive system has not been discussed [20] and it lacks the torque ripple comparisons. In [21], SPWM and SVPWM have been compared and SVPWM has been found to have higher DC link utilization rate and less switching losses. However, the study lacks comparisons of the THIPWM. Space vector pulse width modulation and THIPWM have been compared in [22], but the results associated with THD values of current waveforms have not been clearly demonstrated as it has not been tested on a motor drive system. The comparative study in [23] does not contain the resultant influence of PWM strategies on torque ripples for IPM drives and the study lacks SVPWM comparisons. Similarly, [24] lacks SVPWM comparisons. To the best of authors' knowledge, there is no detailed comparison of SPWM, THIPWM, and SVPWM strategies on the IPM drive in the literature. Thus, this study compares SPWM, THIPWM, and SVPWM strategies in detail in an IPM drive system.

II. MATHEMATICAL EXPRESSIONS

According to Fig. 1, coordinate transformations are applied and the motor is modelled on the dq-axes so that the IPM can be controlled similar to direct current motors. In (1)–(3), electrical equations are given [25].

$$V_d = R_s * I_d + L_d * \frac{dI_d}{dt} - w_e * L_q * I_q \quad (1)$$

$$V_q = R_s * I_q + L_q * \frac{dI_q}{dt} + w_e * L_d * I_d + w_e * \Psi_m \quad (2)$$

$$T_e = \frac{3 * p}{2} * (I_q * \Psi_m + (L_d - L_q) * I_d * I_q) \quad (3)$$

The expression of the stator current according to the currents in the d- and q- axes is as in (4–6).

$$I_d = -I_s * \sin\beta \quad (4)$$

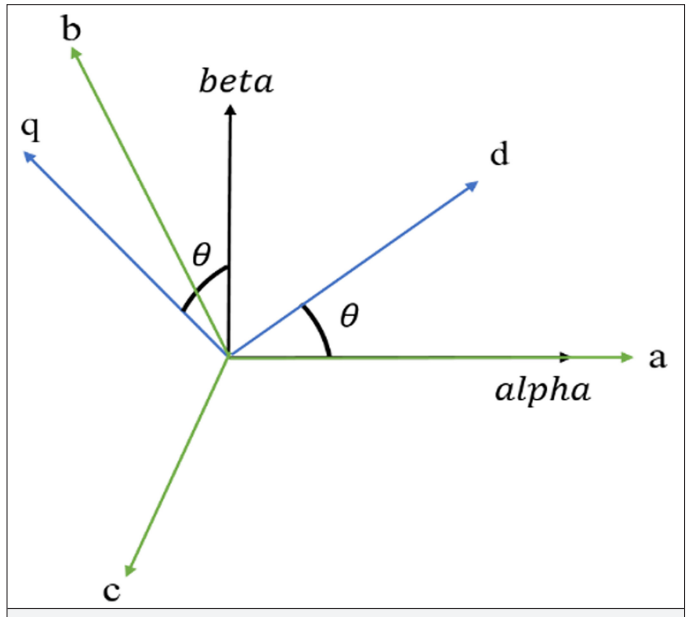

Fig. 1. Coordinate transformations.

$$I_q = I_s * \cos\beta \quad (5)$$

$$|I_s| = \sqrt{I_d^{\,2} + I_q^{\,2}} \quad (6)$$

The schematic of the drive system is shown in Fig. 2. As given in Fig. 2, after the command current values received from the polar to Cartesian block and the dq-axes current values measured from the motor phases are regulated by Proportional Integral (PI) regulators and voltage commands are obtained in the d- and q-axes to be fed to the PWM strategy block.

The transient performance of the drive system is improved by eliminating the coupling terms in the motor model with the decoupling compensation [26]. In addition, the voltage is limited with the overmodulation strategy to the maximum available DC-link voltage based on the PWM strategy adopted in the drive system. Hence, the simulated IPM drive better represents the real-world machine drive system.

The θ angle is obtained from the instantaneous position information of the rotor. While it can be obtained by using an encoder or a resolver depending on the drive design, there are studies that enable the θ angle to be found by using sensorless control techniques [27]. However, it is noteworthy that the sensorless drives, in general, suffer from inaccurate position estimation at low speeds. In this paper, the accurate rotor position angle has been employed in the transformations similar to the drives with an encoder.

A. Implementation of PWM Strategies in IPM Drive System

The fundamental theory associated with the PWM strategies can be found in [28].

1) Sinusoidal Pulse Width Modulation

The SPWM strategy works on the principle of comparing the low-frequency sine waves to be modulated with the high-frequency triangle wave. If the instantaneous value of the high-frequency wave is greater than the amplitude of the signal to be modulated, the output

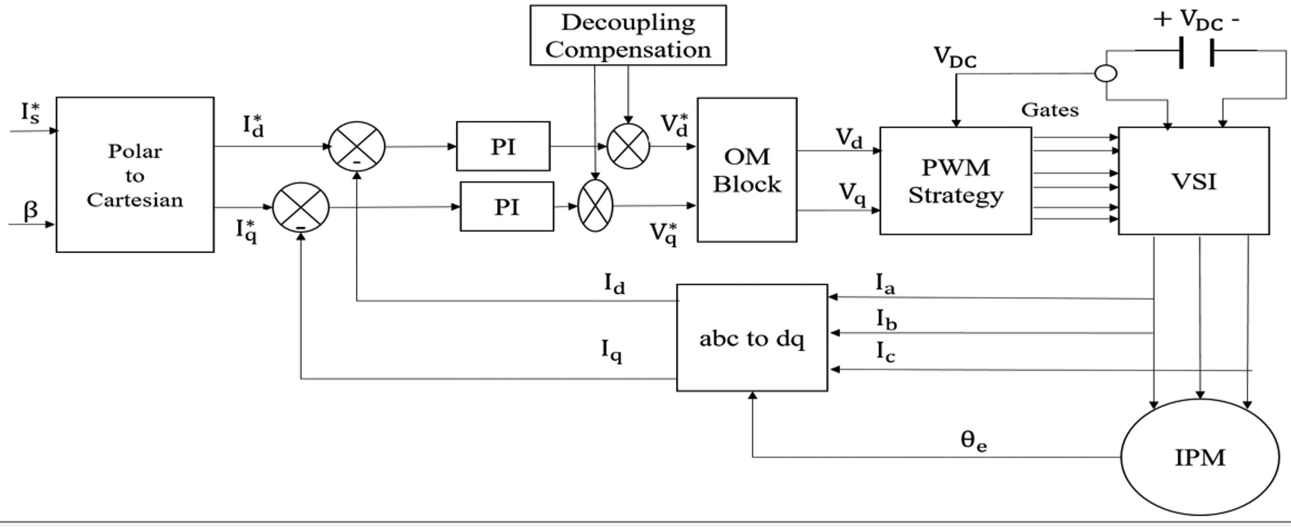

Fig. 2. Schematic of IPM drive system setup.

will be 0, otherwise it will be 1. The modulation index of SPWM is given in (7).

$$m = \frac{V_{modulated}}{V_{carrier}} \tag{7}$$

The signal to be modulated is obtained by converting the voltage values on the dq-axes from the position information of the motor into three-phase sine waves on the abc axes with the help of Clark and Park transformations. dq-axes to abc axes transformation matrix is given in (8). As can be seen from Fig. 2, dq-axes voltage values obtained from PI regulators are transformed into abc axes with the inverse of Clark and Park matrices in PWM strategies block. Then, PWM signals are obtained by comparing them with a high-frequency carrier signal. The theory of the SPWM technique and its implementation strategy with further detail can be found in [29].

$$\begin{bmatrix} V_a \\ V_b \\ V_c \end{bmatrix} = \begin{bmatrix} \cos\theta & -\sin\theta \\ \cos\theta - \frac{2*\pi}{3} & -\sin\theta - \frac{2*\pi}{3} \\ \cos\theta + \frac{2*\pi}{3} & -\sin\theta + \frac{2*\pi}{3} \end{bmatrix} \begin{bmatrix} V_d \\ V_q \end{bmatrix} \tag{8}$$

2) Third Harmonic Injection Pulse Width Modulation

This method has been developed as a solution to the low DC link utilization problem of the SPWM strategy. Third harmonics are injected into the signal to be modulated in this strategy. The scalar "K" factor before the trigonometric expressions in THIPWM voltage equations allows the inverter to use higher DC link voltage. The "K" scalar factor is expressed as in (9), and as can be seen from (9), THIPWM ~15.5% increases the DC link voltage utilization rate than SPWM. Since the THIPWM strategy is based on SPWM, the implementation technique is the same as SPWM. Injection of third harmonic components into reference signals in (10–12) is the difference of the strategy from SPWM. Further details and implementation of strategy can be found in [22].

$$K = \frac{2}{\sqrt{3}} = 1.154 \tag{9}$$

The voltage equations of the waves to be modulated are given in (10–12).

$$V_{an} = 1.154*\left(\sin\theta + \frac{1}{6}\sin 3\theta\right) \tag{10}$$

$$V_{bn} = 1.154*\left(\sin\left(\theta - \frac{2\pi}{3}\right) + \frac{1}{6}\sin 3\theta\right) \tag{11}$$

$$V_{bn} = 1.154*\left(\sin\left(\theta + \frac{2\pi}{3}\right) + \frac{1}{6}\sin 3\theta\right) \tag{12}$$

3) Space Vector Pulse Width Modulation

SPWM and THIPWM strategies modulate sinusoidals by transforming the dq-axes voltages produced by the PI regulators to the abc axes. However, in the SVPWM strategy, the dq-axes voltages obtained from the PI regulators are transformed into the $\alpha\beta$ stationary frame, and the reference vector rotating inside the hexagonal structure in Fig. 3 is obtained. The time durations to be used in switching and the modulation index are calculated from the amplitude and angle information of the reference vector. T_0, T_1, and T_2 are obtained as in (13–15) from the information in which sector the reference vector lies [30].

$$T_1 = m*T_s*\sin\left(\left(n*\frac{\pi}{3}\right) - \theta\right) \tag{13}$$

$$T_2 = m*T_s*\sin\left(\theta - (n-1)*\frac{\pi}{3}\right) \tag{14}$$

$$T_0 = T_s - (T_1 + T_2) \tag{15}$$

θ, n, m, and T_s are the angle of reference vector, sector number, modulation index, and sampling time, respectively. Modulation index is given by (16).

$$m = \frac{\sqrt{3}*V_{ref}}{V_{DC}} \tag{16}$$

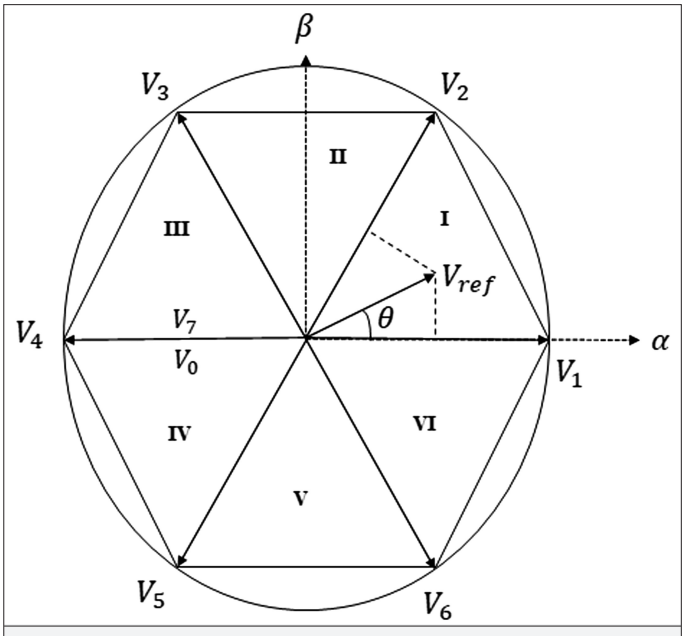

Fig. 3. Hexagonal structure.

V_{ref} and V_{DC} are reference vector amplitude and DC link voltage, respectively. Switching time durations for each sector are stored as look-up tables so that the minimum switching can be achieved in SVPWM strategy [30]. Even though the DC link voltage utilization rates are the same with the THIPWM and SVPWM strategies, implementation of SVPWM strategy is more complicated. However, the output waveforms are smoother since SVPWM strategy updates only one switch in each period.

Firstly, dq-axes reference voltage values are obtained in $\alpha\beta$ frame via inverse Clark matrix. Then the amplitude of the reference vector and the angle of rotation in the hexagon are determined. As can be seen from Fig. 4, the sector number and the time durations for each sector are obtained. After the signal to be modulated is generated, PWM signals are obtained by comparing it with the high-frequency carrier wave. Further details and detailed implementation strategy can be found in [30].

III. SIMULATION IMPLEMENTATION OF DRIVE SYSTEMS AND COMPARATIVE STUDIES

As has been discussed, the voltages in the drive system are limited according to the PWM strategy. In theory, while the SPWM strategy uses 50% of the available DC-link voltage, the THIPWM and SVPWM strategies can use ~57.7% of the DC-link voltage. These percentages come from the fact that SVPWM and THIPWM use ~15.5% more DC-link voltage than SPWM. The switching frequency of the simulated IPM drives for each PWM strategy is 8 kHz for fair comparisons. The parameters of the IPM motor used in the simulations are listed in Table I. The schematic of the simulated drive system is shown in Fig. 5.

TABLE I. MOTOR PARAMETERS

Motor Type	Interior Mounted Permanent Magnet Synchronous Motor
Pole Num.	8
L_d	0.846 mH
L_q	1.656 mH
R_s	0.0463 ohm

A. Validation of IPM Drives with SPWM, THIPWM, and SVPWM Strategies

IPM drive systems have been implemented by employing three different PWM strategies and each drive has been validated through extensive simulations. The mechanical speed has been increased from stand-still to 1500 rpm in 0.3 seconds in a linear form and it was kept constant at 1500 rpm till 0.5 seconds in the simulated drives. It is evident in Fig. 6 that the control system achieves accurate torque control in steady states as well as in transient states with all three PWM strategies. As can be seen from Fig. 6, the drive systems are robust when operating torque and speed are varied.

One can deduce from Fig. 6 that the SVPWM strategy produces less torque ripple. Details and further comparisons will be made in the following sections.

B. Total Harmonic Distortion Comparison of Drives

THD rates of the drives with the three different PWM strategies are compared, and the results at different speed and torque operating points are listed in this section. The comparative results at 500 rpm, 1000 rpm, and 1500 rpm are illustrated in Fig. 7 when the electromagnetic torque production is 10, 20, and 30 Nm. Hence, the THD comparisons are made at wide range. It is evident in Fig. 7 that the lowest THD rate is obtained at any operating point when SVPWM strategy is adopted, whereas the distortion rate is the highest when SPWM strategy is adopted. This implies that the SVPWM strategy is the best among others in terms of current harmonic distortion. Accordingly, reduced torque ripple can be achieved by adopting SVPWM strategy in modern drives. It is noteworthy that THD ratios reduce in each PWM strategy in Fig. 7 when torque reduces, and speed is constant. This is as expected since the current magnitude increases with

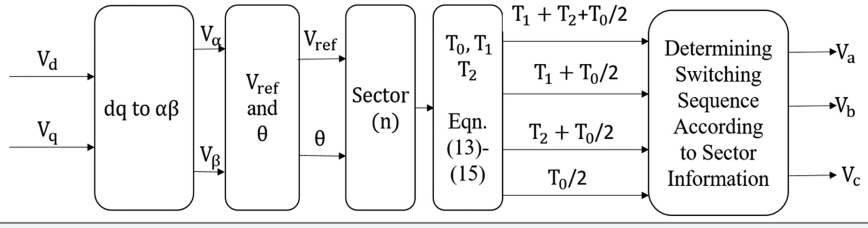

Fig. 4. SVPWM schematic.

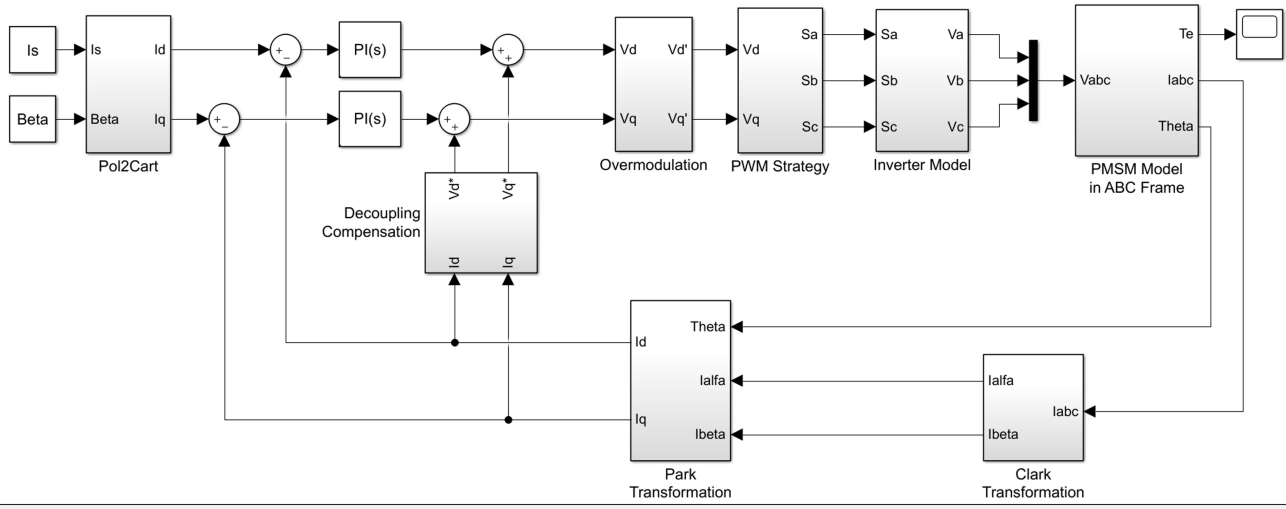

Fig. 5. The schematic of the simulation (in Matlab/Simulink©).

the increasing torque and hence the ratio is relatively lower. In contrast, THD ratios increase in each PWM strategy when torque is constant, and speed increases. This is also as expected since the switching is more frequently updated with the increasing electrical frequency.

C. Comparisons of Torque Outputs and Phase Currents Waveforms

The three PWM strategies have been tested on the drive systems, and the comparisons of output torque and phase current waveforms have been made in this section. In Fig. 8, while the mechanical speed value is 500 rpm, 1000 rpm, and 1500 rpm, three different torque values, 10,

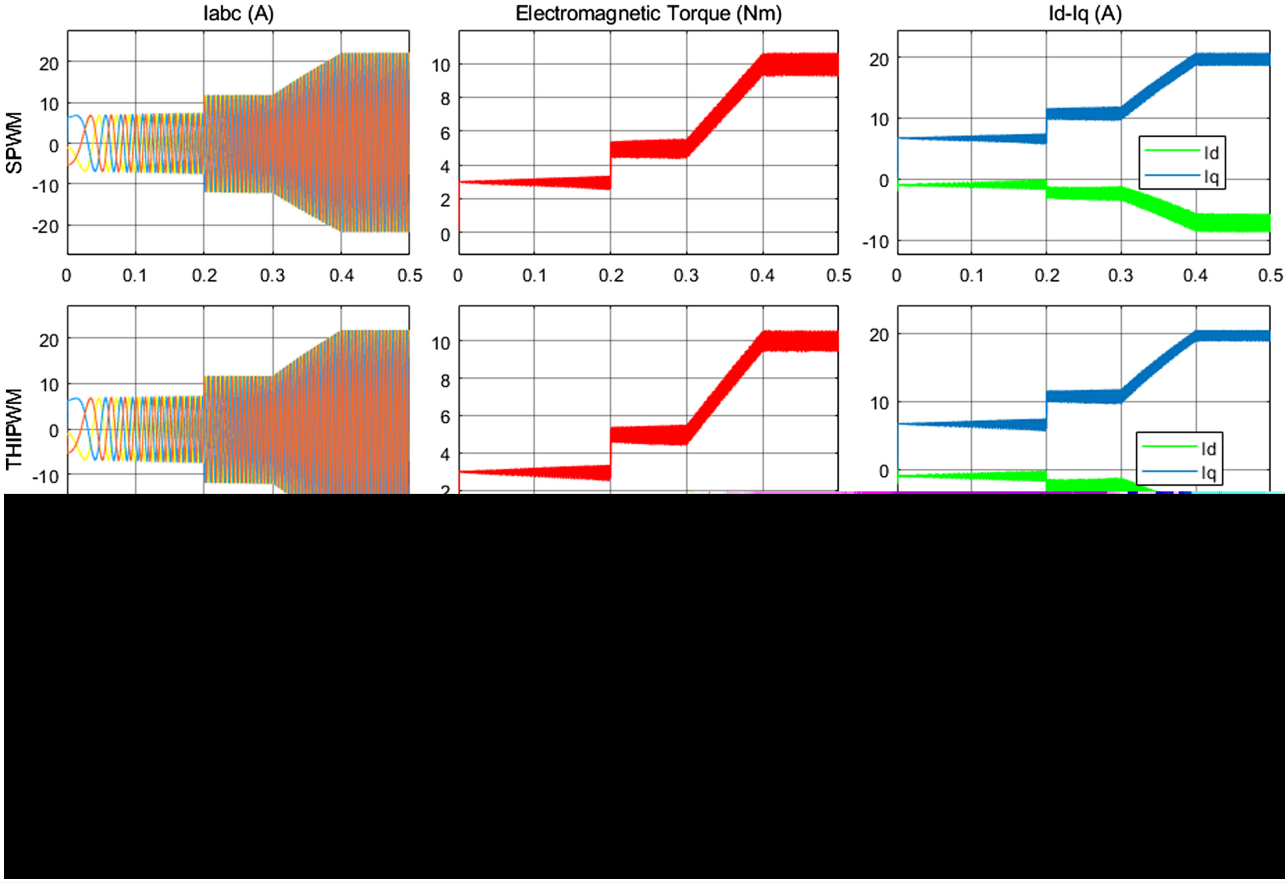

Fig. 6. IPM drive system validation with different PWM strategies.

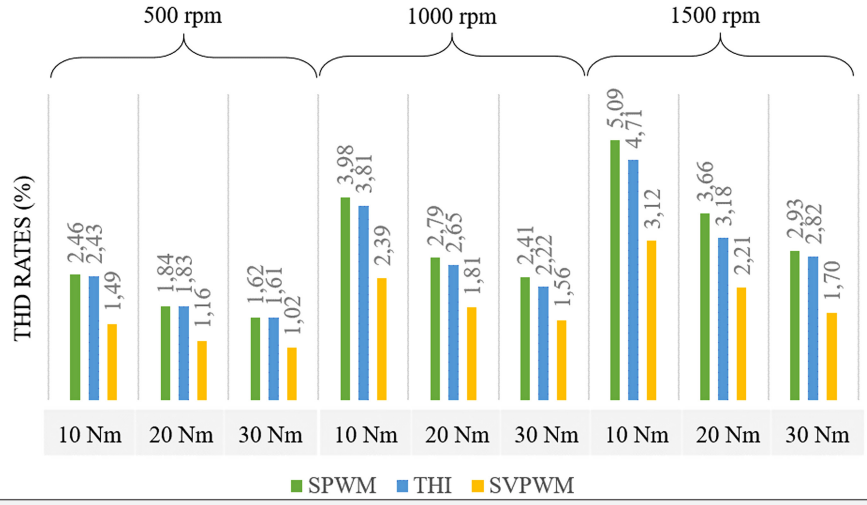

Fig. 7. Comparisons of THD rates with different switching strategies.

20, and 30 Nm, have been tested and torque ripple values have been plotted on the same graph so that the ripple comparisons can be seen clearly. It is evident from the results that when the SVPWM strategy is adopted as a modulation technique, the produced output torque is the smoothest compared to produced electromagnetic torque waveforms obtained with SPWM and THIPWM strategies. It is also seen from the results that the torque waveforms obtained with the THIPWM have less ripple than the results obtained with SPWM strategy, and hence, the SPWM strategy increases the torque ripple at wide range of operation. The results are coherent with the THD ratios obtained in the

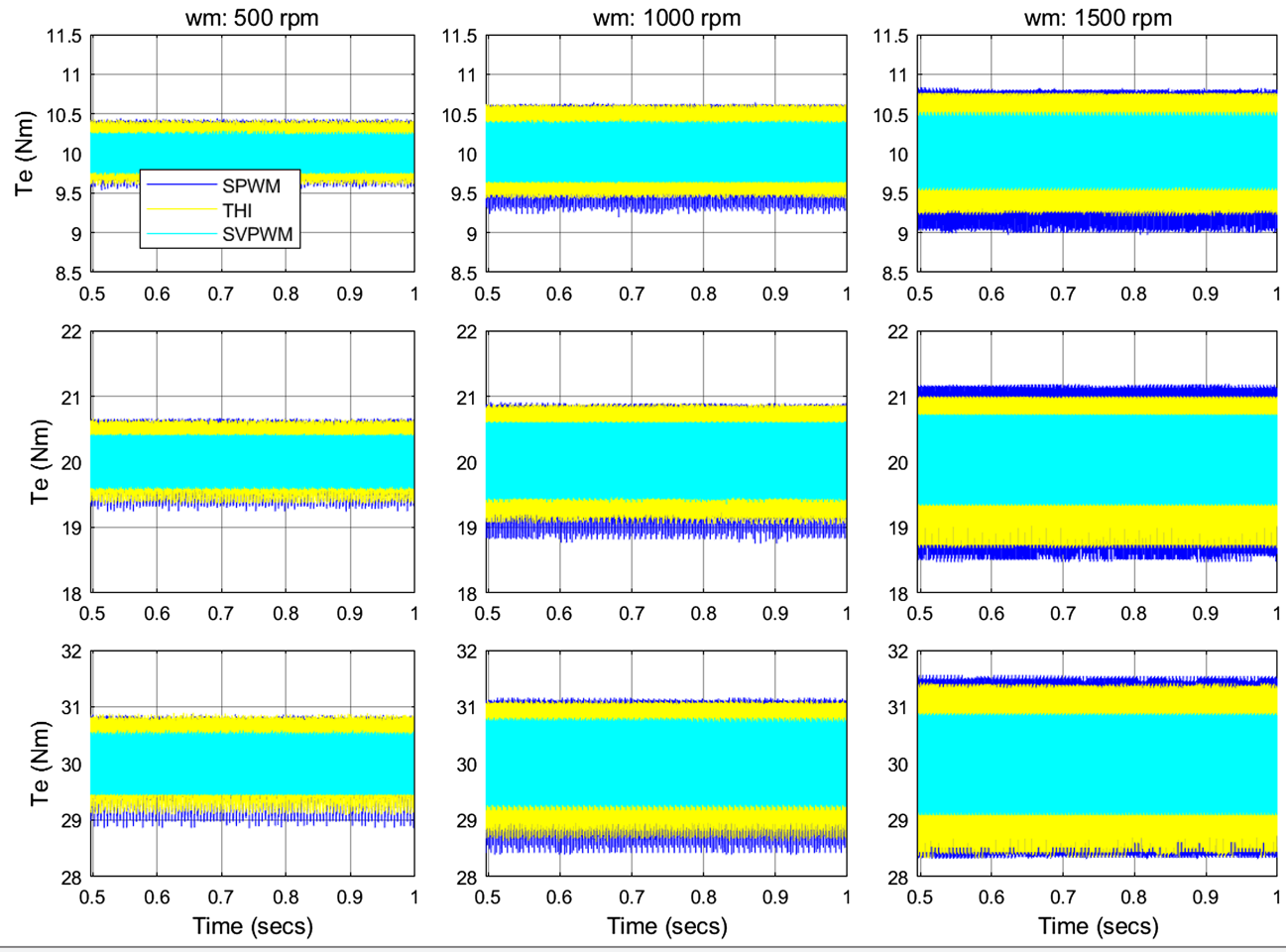

Fig. 8. Comparisons of torque ripples for each PWM strategies.

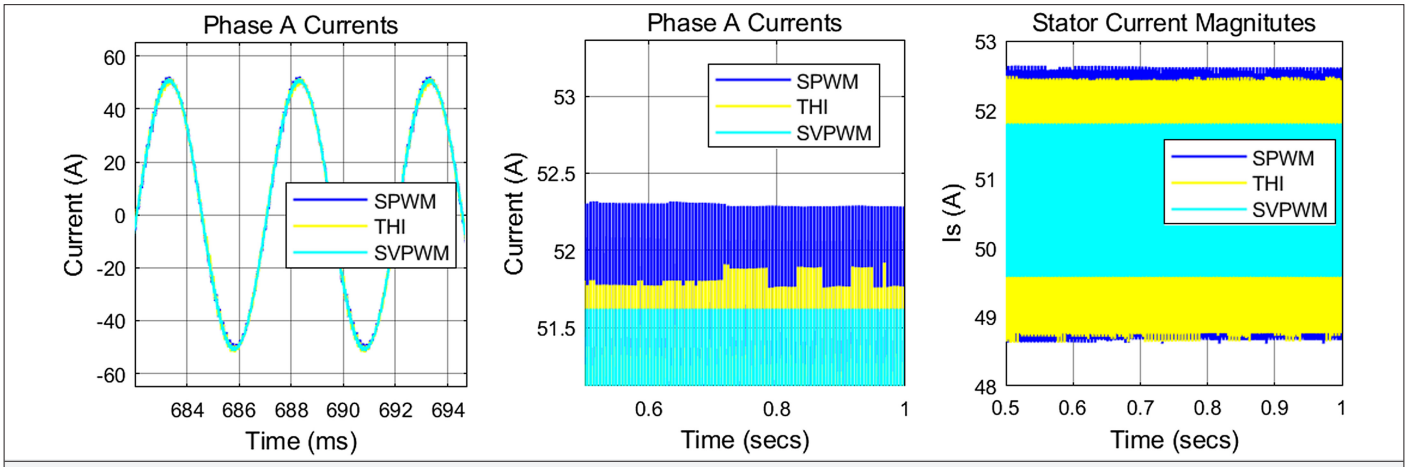

Fig. 9. Phase current comparisons for each PWM strategy.

previous section. It is noteworthy that when the drives with SPWM and SVPWM strategies operate at 1500 rpm speed and 30 Nm torque, the ripple on the output torque waveforms is ~3 Nm and ~2 Nm, respectively. This implies that the undesired ripple ratio can be significantly improved by adopting the SVPWM strategy in modern drives.

Fig. 9 illustrates the phase current waveforms of the drives when the machine operates at 1500 rpm mechanical speed and 30 Nm electromagnetic torque. As will be seen from Fig. 9, phase currents of the drive employing the SVPWM strategy have less distortion, whereas the distortion on the current waveforms is the worst when the SPWM strategy is adopted. The increased distortion of the current waveforms directly increases the output torque ripple as evident in Fig. 8.

IV. CONCLUSIONS

In this study, three different PWM strategies (SPWM, THIPWM, and SVPWM) commonly used in recent AC drives have been compared in IPM drives when the machine operates at different points. Comprehensive simulations have been performed at different mechanical speeds and electromagnetic torque values. The results validate that SPWM is not a suitable modulation technique for modern drives as its DC link voltage utilization rate is lower than SVPWM and THIPWM and the current distortions and the torque ripples are the highest with SPWM. Although THIPWM utilizes the DC link voltage at higher levels, it lags behind SVPWM in terms of torque ripple and stator current distortion ratio. As a result of the simulations, torque ripple ratios of SPWM, THIPWM, and SVPWM strategies have been obtained as at 1500 rpm and 30 Nm torque as 4.94%, 4.45%, and 2.81%, respectively. The torque ripple ratio of the SVPWM strategy at this operating point is 43% and 36.85% lower than the SPWM and THIPWM strategies, respectively. Hence, the SVPWM strategy gives the best result in terms of THD ratios at wide operation range among all three strategies and it achieves the smoothest torque production. In the light of the results, SVPWM strategy is the most suitable modulation strategy for modern IPM drives.

Peer-review: Externally peer-reviewed.

Author Contributions: Concept – O.E.Ö., M.K.; Design – O.E.Ö., M.K.; Supervision – M.K.; Materials – O.E.Ö., M.K.; Data Collection and/or Processing – O.E.Ö., M.K.; Analysis and/or Interpretation – O.E.Ö., M.K.; Literature Review – O.E.Ö., M.K.; Writing – O.E.Ö., M.K.; Critical Review – O.E.Ö., M.K.

Declaration of Interests: The authors have no conflicts of interest to declare.

Funding: This study has been supported by the Scientific and Technological Research Council of Turkey (TUBITAK) through the Scientific and Technological Research Projects Funding Program (1001) with a project numbered 118E858.

REFERENCES

1. Z. Wang, T. W. Ching, S. Huang, H. Wang, and T. Xu, "Challenges faced by electric vehicle motors and their solutions," in *IEEE Access*, vol. 9, pp. 5228–5249, 2021. [CrossRef]
2. Z. Zhang et al., "A deadbeat PI controller with modified feedforward for PMSM under low carrier ratio," in *IEEE Access*, vol. 9, pp. 63463–63474, 2021. [CrossRef]
3. G. Liu, G. Xu, W. Zhao, X. Du, and Q. Chen, "Improvement of torque capability of permanent-magnet motor by using hybrid rotor configuration," in *IEEE Trans. Energy Convers.*, vol. 32, no. 3, pp. 953–962, 2017. [CrossRef]
4. J. Hang et al., "Integration of Interturn Fault diagnosis and torque ripple minimization control for direct-torque-controlled SPMSM drive system," in *IEEE Trans. Power Electron.*, vol. 36, no. 10, pp. 11124–11134, Oct. 2021. [CrossRef]
5. Y. Zhang, Z. Yin, C. Bai, G. Wang, and J. Liu, "A rotor position and speed estimation method using an improved linear extended state observer for IPMSM sensorless drives," in *IEEE Trans. Power Electron.*, vol. 36, no. 12, pp. 14062–14073, 2021. [CrossRef]
6. H. Li, Z. Wang, Z. Xu, X. Wang, and Y. Hu, "Feedback linearization based direct torque control for IPMSMs," in *IEEE Trans. Power Electron.*, vol. 36, no. 3, pp. 3135–3148, 2021. [CrossRef]
7. M. Koç, T.Sun, and J. Wang, "Performance improvement of direct torque controlled interior mounted permanent magnet drives by employing a linear combination of current and voltage based flux observers," *IET Power Electron.*, vol.9, no.10, pp. 2052–2059, 2016. [CrossRef]
8. S. J. Kim, J. -W. Kim, B. -G. Park, and D. -H. Lee, "A novel predictive direct torque control using an optimized PWM approach," in *IEEE Trans. Ind. Appl.*, vol. 57, no. 3, pp. 2537–2546, May–June 2021. [CrossRef]
9. X. Wang, Z. Wang, and Z. Xu, "A hybrid direct torque control scheme for dual three-phase PMSM drives with improved operation performance," in *IEEE Trans. Power Electron.*, vol. 34, no. 2, pp. 1622–1634, Feb. 2019. [CrossRef]
10. C. Liu, and J. Shang, "Sensorless drive strategy of open-end winding PMSM with zero-sequence current suppression," in *IEEE Trans. Energy Convers.*, vol. 36, no. 4, pp. 2987–2997, 2021. [CrossRef]
11. R. K. Mahto, A. Mishra, and R. C. Bansal, "A reduced switch five-level VSI for high-performance vector controlled PMSM drive," *Electr. Power Compon. Syst.*, vol. 48, no. 12–13, pp. 1433–1443, 2020. [CrossRef]
12. S. Albatran, A. S. Allabadi, A. R. A. Khalaileh, and Y. Fu, "Improving the performance of a two-level voltage source inverter in the overmodulation region using adaptive optimal third harmonic injection pulsewidth modulation schemes," in *IEEE Trans. Power Electron.*, vol. 36, no. 1, pp. 1092–1103, 2021. [CrossRef]

13. S. Albatran, A. R. A. Khalaileh, and A. S. Allabadi, "Minimizing total harmonic distortion of a two-level voltage source inverter using optimal third harmonic injection," in *IEEE Trans. Power Electron.*, vol. 35, no. 3, pp. 3287–3297, 2020. [CrossRef]
14. E. Oksuztepe, Z. Omaç, and H. Kurum, "Sensorless vector control of PMSM with non-sinusoidal flux using observer based on FEM," *Electr. Eng.*, vol. 96, no. 3, pp.227–238, 2014. [CrossRef]
15. K. Saleh, and M. Sumner, "Sensorless speed control of a fault-tolerant five-phase PMSM drives," *Electr. Power Compon. Syst.*, vol. 48, no. 9-10, pp.919–932, 2020. [CrossRef]
16. Y. Ge, L. Yang, and X. Ma, "Adaptive sliding mode control based on a combined state/disturbance observer for the disturbance rejection control of PMSM," *Electr. Eng.*, vol. 102, no. 4, pp. 1863–1879, 2020. [CrossRef]
17. R. Sarker, A. Datta, and S. Debnath, "FPGA-based high-definition SPWM generation with harmonic mitigation property for voltage source inverter applications," in *IEEE Trans. Ind. Inform.*, vol. 17, no. 2, pp. 1352–1362, 2021. [CrossRef]
18. W. Liao, M. Lyu, S. Huang, Y. Wen, M. Li, and S. Huang, "An enhanced SVPWM strategy based on vector space decomposition for dual three-phase machines fed by two DC-source VSIs," in *IEEE Trans. Power Electron.*, vol. 36, no. 8, pp. 9312–9321, 2021. [CrossRef]
19. H. Yao, Y. Yan, T. Shi, G. Zhang, Z. Wang, and C. Xia, "A novel SVPWM scheme for field-oriented vector-controlled PMSM drive system fed by cascaded H-bridge inverter," in *IEEE Trans. Power Electron.*, vol. 36, no. 8, pp. 8988–9000, 2021. [CrossRef]
20. B. Chokkalingham, S. Padmanaban, and F. Blaabjerg, "Investigation and comparative analysis of advanced PWM techniques for three-phase Three-Level NPC-MLI drives," *Electr. Power Compon. Syst.*, vol. 46, no. 3, pp.258–269, 2018. [CrossRef]
21. B. Tian, M. Molinas, and Q. An, "PWM investigation of a field-oriented controlled five-phase PMSM under two-phase open faults," in *IEEE Trans. Energy Convers.*, vol. 36, no. 2, pp. 580–593, 2021. [CrossRef]
22. B. Tan, Z. Gu, K.Shen, and X. Ding, "Third harmonic injection SPWM method based on alternating carrier polarity to suppress the common mode voltage," in *IEEE Access*, vol. 7, pp. 9805–9816, 2019. [CrossRef]
23. N. K. Muthukuri, and S. Mopidevi, "Analysis of a modified switching pattern for packed U Cell-15 inverter topology with advanced level shift carrier pulse width modulation techniques, " *Electrica*, vol. 21, no. 2, pp. 272–282, 2021. [CrossRef]
24. N. Sujitha, S. S. Kumar, and M. Sasikumar, "Design and implementation of hybrid SPWM control for Cascaded H-bridge multi level inverter for motor drives," *Electrica*, vol. 14, pp. 1721–1727, 2014.
25. G. Feng, C. Lai, X.Tan, and N. C. Kar, "Maximum-torque-per-square-ampere control for interior PMSMs considering cross-saturation inductances," in *IEEE Trans. Transp. Electrif.*, vol. 7, no. 3, p. 1482–1492, 1492. [CrossRef]
26. T. Sun, M. Koç, and J. Wang, "MTPA control of IPMSM drives based on virtual signal injection considering machine parameter variations," in *IEEE Trans. Ind. Electron.*, vol. 65, no. 8, pp. 6089–6098, 2018. [CrossRef]
27. G. Wang, M. Valla, and J. Solsona, "Position sensorless permanent magnet synchronous machine drives—A review," in *IEEE Trans. Ind. Electron.*, vol. 67, no. 7, pp. 5830–5842, 2020. [CrossRef]
28. S.-H. Kim, "Pulse width modulation inverters, ", in *Electric Motor Control.* Netherlands: Elsevier Science, 2017, pp. 265–340.
29. M. Lakka, E. Koutroulis, and A. Dollas, "Development of an FPGA-based SPWM generator for high switching frequency DC/AC inverters," in *IEEE Trans. Power Electron.*, vol. 29, no. 1, pp. 356–365, 2014. [CrossRef]
30. G.-M. Sung, W.-Y. Wang, and H.-Y. Hsieh, "Chip implementation of digital scalar space-vector pulse width modulation for induction motor drive," *Electr. Power Compon. Syst.*, vol. 39, no. 16, pp. 1733–1747, 2011. [CrossRef]

Osman Emre Özçiflikçi was born in Turkey. He received the BSc and MSc degrees from Erciyes University, Kayseri, Turkey, in 2019 and in 2021, respectively, both in Electrical and Electronics Engineering where he is currently pursuing the PhD degree. He is a Research Assistant in Electrical and Electronic Engineering Department in Engineering Faculty at Kirsehir Ahi Evran University. His research interests include electrical machines and AC drives.

Mikail Koç was born in Turkey. He received the BSc degree from ESOGU University, Eskisehir, Turkey, in 2009, the MSc degree from Nottingham University, UK, in 2012, and the PhD degree from the University of Sheffield, UK, in 2016 all in Electrical and Electronic Engineering. He is currently an Assistant Professor in Electrical and Electronic Engineering Department in Engineering Faculty at Kirsehir Ahi Evran University. His research interests include advanced control strategies for electric drives.